Control of cultured human cells with femtosecond laser ablated patterns on steel and plastic surfaces

Tarmo Nuutinen · Martti Silvennoinen ·
Kimmo Päiväsaari · Pasi Vahimaa

Abstract The purpose of the present study is to explore topographical patterns produced with femtosecond laser pulses as a means of controlling the behaviour of living human cells (U2OS) on stainless steel surfaces and on negative plastic imprints (polycarbonate). The results show that the patterns on both types of material strongly affect cell behaviour and are particularly powerful in controlling cell spreading/elongation, localization and orientation. Analysis by fluorescence and scanning electron microscopy shows that on periodic 1D grating structures, cells and cell nuclei are highly elongated and aligned, whereas on periodic 2D grid structures, cell spreading and shape is affected. The results also show that the density and morphology of the cells can be affected. This was observed particularly on pseudo-periodic, coral-like structures which clearly inhibited cell growth. The results suggest that these patterns could be used in a variety of applications among the fields of clinical research and implant design, as well as in diagnosis and in cell and drug research. Furthermore, this article highlights the noteworthy aspects and the unique strengths of the technique and proposes directions for further research.

Keywords Laser ablation · Stainless steel · Polycarbonate · Hierarchical surface structures · Cell behaviour · Human cells

T. Nuutinen (✉)
Department of Biology, University of Eastern Finland,
PO Box 111, FI-80101 Joensuu, Finland
e-mail: tarmo.nuutinen@uef.fi

M. Silvennoinen · K. Päiväsaari · P. Vahimaa
Department of Physics and Mathematics,
University of Eastern Finland,
PO Box 111, FI-80101 Joensuu, Finland

1 Introduction

Biomaterial-cell interaction is one of the key issues in life sciences and it is currently under extensive study (Huebsch et al. 2009). Numerous factors affect the interaction of a man-made scaffold and cells. Therefore, basic multidisciplinary research is needed prior to clinical trials for, for example, the implantation of bone replacements or the introduction of new electronic devices into the human body. In addition to promoting tissue growth and healing, or the integration of these devices by facilitating cell adhesion, the guidance of living cells by structural cues may have further applications among other fields in life sciences, such as cellular and molecular biology (Huebsch et al. 2009). For example, a living cell-based assay could benefit from cell growth control, especially if applicable in high-throughput formats. This could be a plastic microtiter plate providing niches for cells or a "cells on a chip" microchip array (El Ali et al. 2006) for miniaturized cell cultures and single cell analysis, in combination with a microfluidistic system (Zare et al. 2010). Such a system could be used for, for example, drug screening and discovery, or contribute to the development of single cell bio-devices (Sato et al. 2009). For the pursuit of longer-term goals in tissue engineering it would provide scaffold for studying stem cell differentiation (Mei et al. 2007; Underhill et al. 2007) or could be employed in diagnostics.

Similar to other physicochemical properties of the surface or the matrix, topographies have a major impact on cell behaviour (Lim et al. 2007; Meyer et al. 2005). Structures such as grooves, pits and arrays of pillars have been produced by various methods in order to control cell behaviour (Schmidt et al. 2009). Examples of this include using electron beam lithography followed by solvent casting structures on polystyrene, which has been used in the study of fibroblast alignment (Loesberg et al. 2007), or using direct electron beam evaporation in order to generate nano- and micro-structures for directing cells (Puckett et al. 2008). Additionally, there are a vast

number of alternatives to expensive electron beam lithography. The two most well-known alternatives are photolithography and soft lithography. In combination with other techniques, imprinting (Truskett et al. 2006) or soft lithography is typically used in micron scale chemical patterning (Qin et al. 2010). Whatever the approach or the methods may be, the purpose is to control cell behaviour; differentiation, migration, proliferation or spreading. For example, the control of cell spreading and orientation is crucial, especially in the development of certain tissues and in cell differentiation, for example in nerve regeneration (Recknor et al. 2006) or in the coating of vascular grafts with endothelial cells (Uttayarat et al. 2005).

Femtosecond laser ablation is a versatile tool for the generation of both self-organized and directly written nano-, micro- and macrostructures, basically on any material and without photomasks or specialized environments. Using other methods, the producing of multilevel structures can be time-consuming and expensive. Laser ablation, however, is capable of generating large uniform areas even in a single manufacturing step in ambient conditions (Huang et al. 2008). The attribute of laser ablation that produces Light Induced Periodic Surface Structures (LIPSS) (Qi et al. 2009; Zhao et al. 2007)—in addition to micron scale structures—is yet to be exploited in terms of biomaterials. LIPPS are nanometer scale structures whose orientation can be controlled with the polarization of ablation pulses. The control over nanostructures can be particularly powerful in controlling cell behaviour, but also in altering wetting properties, since wetting is dependent on the structural features of the surface, in addition to the basic chemical properties of the material. For example, specific combinations of micro- and nanostructures on a surface are able to turn a slightly hydrophobic material to "superhydrophobic"—a phenomenon commonly known as the "lotus effect", which has been under extensive investigation for its numerous applications (Zhang et al. 2008). Hence, laser ablation has been applied with this intention as well, and with the method, even a metal surface has been turned into "superhydrophobic" (Kietzig et al. 2009) and a silicon wafer surface to "superhydrophilic" (Vorobyev et al. 2010).

However, only a limited number of studies have so far reported interaction between a laser ablated biomaterial and living cells. Previous studies have shown that laser ablation is a suitable method for optimizing the electrode-cell contact (Reich et al. 2008) and selectivity (Schlie et al. 2009). In the study by Paul et al. (2008), an inflammatory response of macrophages was triggered with topographical cues on polyvinylidene fluoride (PVDF), while Yeong et al. (2010) studied how a microchannel structure directly written on a polymer surface affected cell alignment. The present study, however, presents direct large uniform patterning of stainless steel with femtosecond laser pulses, after which the patterns are hot embossed to polycarbonate (PC). Since

surface energies have an important role in the biological adsorption (Zhang et al. 2008), we have characterized the wetting properties of representative structures. In the second part of the study, we further concentrate on the effects of topographies to cultured human osteosarcoma (U2OS) cell behaviour on both stainless steel surfaces and on their negative imprints on polycarbonate. The present study shows that localization, spreading/elongation, orientation, morphology and cell densities can be affected by surface structures manufactured with this method. The orientation of the cells was controlled especially with multilevel periodic structures, while proliferation was only affected by non- or quasiperiodic structures.

2 Methods

2.1 Fabrication of surface patterns

Prior to surface modifications, the samples of stainless steel M390 alloy (Böhler, purchased from Stén & Co Oy Ab, Nurmijärvi, Finland) were mechanically polished and cleaned with an ultra-sonic bath of acetone and in dH_2O. Gratings were fabricated by irradiating the metal alloy with femtosecond laser pulses (Quantronix Integra C 3,5 mJ, Scanditest Sverige AB, Åkersberga, Sweden), using a width of 120 fs and a 790 nm centre wavelength at up to 1 kHz repetition rate. Multiple 3D motion controllers (Micos Corvus Es 100 and PLS 85) were used in the precise moving of the sample holder.

The surface modifications included pseudo-periodic and periodic structures. The pseudo-periodic structures were fabricated by scanning a focused beam on the surface using a spherical lens with a focal length of 50 mm. The pulse energy used was 1 mJ and the scanning speeds were 14.000, 7.000, 3.500, 1.750, 0.875, 0.438, 0.219, 0.109, 0.055, 0.027 and 0.014 mm/s. The periodic structures were fabricated with a cylinder lens, which produced lines of 15 mm in length and 7 μm in width. Ablating the lines next to each other produced linear gratings with the desired periodicities, 12.5 and 25 μm. For the 2D gratings, perpendicular lines were generated again using 50, 100 or 150 illumination pulses.

Patterned metal plates were then used as moulds when hot-embossing to polycarbonate. Hot-embossing was done using an NIL Eitre 3 tool. Holding time was set to 120 s at 160 °C and in 40 bar pressure.

2.2 Characterization of surface patterns

Micron scale structures were monitored in real time by light microscope, while Light Induced Periodic Surface Structures (LIPSS)—a typical nano-scale roughness in the ablation process—were monitored with a scanning electron

microscope (SEM) (LEO 1550 Gemini). Images presented in Fig. 1a-f have been recorded using a 5.00 kV acceleration voltage and the magnifications 4.51 kX, 895 X, 6.00 kX, 6.19 kX, 1.10 kX and 6.61 kX, respectively.

Structure heights were monitored using a SEM either by making a plastic copy and measuring the height from a cross-section, or by focusing on the highest and deepest points of a metal structure and estimating structure heights from the distance of these measuring points. The wettability properties of the patterned and smooth control surfaces were investigated using an optical contact angle measuring system (KSV Cam200 -camera, KSV Cam2008 -software) at 20 °C, in normal atmospheric conditions, using a droplet size of 5 µl.

2.3 Cell cultures

Osteosarcoma U2 cells (U2OS, ATCC, Manassas VA USA) were selected as a model cell line, since they are well established, and these osteoblast-like cells are known to show moderate variability and matrix producing properties, and no mineralization of the matrix ((ter Brugge et al. 2002) and references within)—all aspects that could be problematic analysing cell growth on highly structural surfaces and by methods used in the present study. The patterned steel samples were sonicated in acetone for 2 h and wrapped in a foil and heat sterilized at 200 °C at least for an hour. The plastic imprints were autoclaved at 121 °C for 20 min. Prior to culturing U2OS cells, the substrates were immersed in

McCoy's5a medium (Lonza, Verviers Belgium), supplemented with 10 % fetal bovine serum, and with 219.15 mg/LL-glutamine (Euroclone, Siziano Italy), and pre-equilibrated at least for 2 h. Pre-wetting was used to ensure uniform distribution of cells on the surfaces, which are known to have a strong effect on fluid behaviour. The starting density of the cultures was 6500 cells/cm^2, since it was found suitable for the employed culture times (48 h or 96 h) and for the both types of substrates.

2.4 Imaging of cell cultures

For the fluorescence microscopy (with Zeiss Axcioplan2 microscope), the cells were washed several times with phosphate-buffered saline (PBS) and fixed with 3 % paraformaldehyde (PFA). The cells were permeabilized for immuno-staining with a 0.1 % Triton-X-100 in PBS. In order to block unspecific binding of antibodies, a 0.2 % gelatin in PBS was used. The primary antibody against β-tubulin (MAB3408) was from Chemicon (Temecula, CA USA). Alexa-fluor conjugated secondary antibodies (A-11029, A-11032), which were used for fluorescent detection of the primary antibody, were purchased from the Molecular Probes (Eugene, OR USA). Final concentrations of all antibodies were 1 µg/mL—only one secondary antibody was used at a time in each experiment (depending on the desired emission wavelength). The nuclei were stained with 1 µg/mL bis-benzimide (Hoechst 33258, Sigma-Aldrich, St. Louis MO USA). In the fluorescence microscope, 20 X,
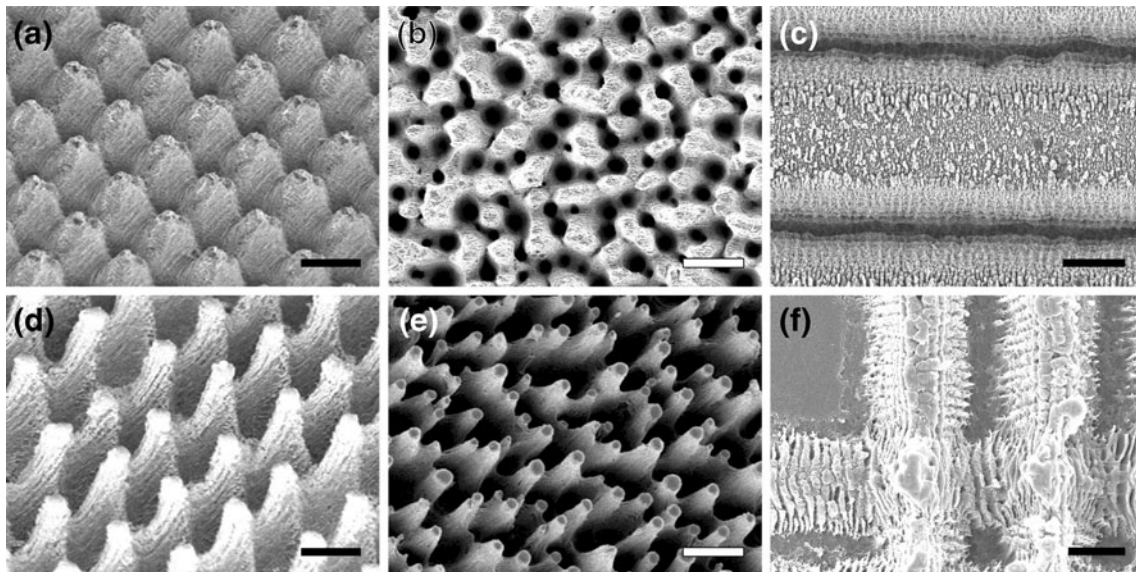

Fig. 1 Laser ablated structures on steel (**a-c**) and hot embossed structures on polycarbonate (**d-f**). 2D periodic grating (**a**) and pseudo-periodic, coral-like (**b**) structures have been hot embossed to polycarbonate (**d** and **e**, respectively). It can be seen that despite the high aspect ratio, the replication process has been carried out without losing any submicron details. **c** A typical 1D grating structure employed in this study. **f** A polycarbonate replica in a position where two 1D gratings cross and form a 2D grating. Bar in **a** and **d** is 10 µm, **b** and **e** 30 µm, **c** 4 µm and **f** 3 µm

10 X and 40 X objective lenses were used for the Figs. 2, 3 and 4, respectively. For the SEM, a drying method presented in (Mata et al. 2002) was used: the cells were fixed with 2 % glutaraldehyde and the water was substituted with ethanol in a step-wise manner (with 50–99.6 % EtOH) and eventually with hexamethyldisilazane (HMDS). After this, the samples were air-dried and preserved in a desiccator until sputter coated with a 15 nm gold layer, using a turbo sputter coater (Emitech K575X, Emitech Limited Ltd, Kent, UK) according to the manufacturer's instructions, and imaging with SEM with acceleration voltage of 5.00 kV and magnifications of 14.23 kX (in Fig. 4c), 80 X (Fig. 5a), 452 X (Fig. 5b), 18.49 kX (Fig. 5c), 4.57 kX (Fig. 5d), 588 X (Fig. 5e) and 1.67 kX (Fig. 5f). After this, some of the samples were stained with 1 μg/mL bis-benzimide and 10x SYPRO Orange (BIORAD, Hercules CA USA) and examined and photographed in a fluorescence microscope.

2.5 Image analysis

The CellProfiler program (Jones et al. 2008) was used to determine the cell densities and the orientation of the nuclei from the fluorescence microscope images of the bis-benzimide stained samples. The nuclei were identified and their number and other parameters were calculated by the program. In three parallel experiments, the orientations of 1052, 1110 and 1009 nuclei were calculated: the experiments were done for the linear gratings with both 12.5 μm and 25 μm periodicity and also for the flat control surfaces of same material, respectively. Standard deviations are shown as error bars in Fig. 3c. To estimate the inhibition of the growth rate of the coral-like structures, a total of 2068 cells were analyzed from four parallel experiments.

3 Results

3.1 Laser ablation, imprinting and material characterization

The introduced topographical changes alter the surface properties of a material. Surfaces with certain combinations of nano and micro structures can exhibit extraordinary wettability; often referred as superhydrophobicity or superhydrophilicity. This is also the case for many different types of laser ablated structures. In this study, contact angle measurements were carried out to find out whether our structures
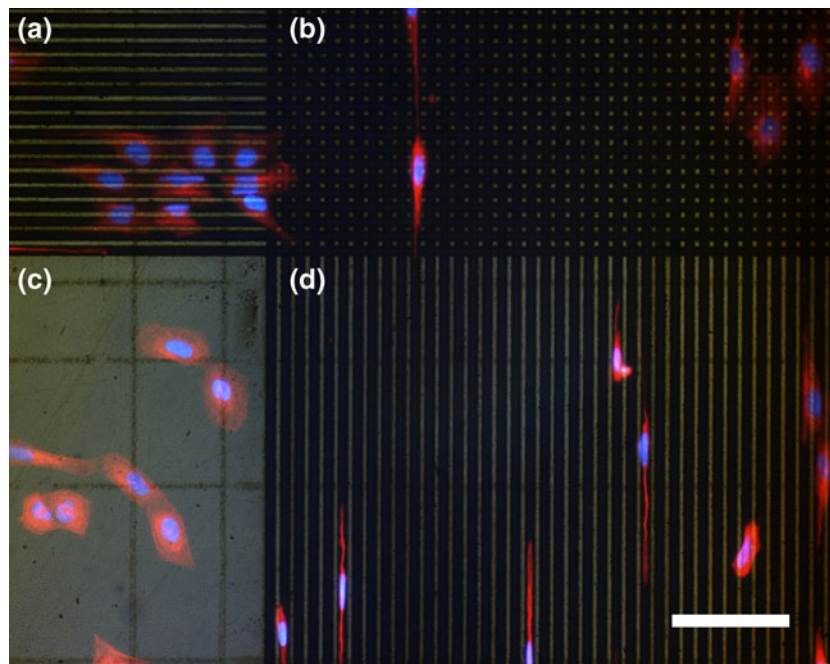

Fig. 2 A typical fluorescence microscope image of cultured U2OS human cells on a steel substrate after 2 days. Structures on the steel are visualized in an epifluorecence microscope without applying filters—the image is merged with blue and red emission channels representing nuclei and β-tubulin networks, respectively. The typical cell morphologies of U2OS cells on a smooth steel surface can be seen in area C. On this substrate, other areas consist of 'horizontal' lines (**a**) and 'vertical' lines (**d**) crossing to form a 2D grid structure (**b**). LIPPS nanogrooves can be either parallel to micron grooves (**d**) or perpendicular to micron grooves (**a**). Hence, all nanogrooves are orientated vertically in this picture—and also in the grid structure (**b**). The height of the grooves in A and D is 4 μm, and hence the height of the structures on the area B varies up to 8 μm. The orientation of LIPPS may in part explain why the cells are more elongated in area D than in A and prefer 'vertical' orientation on the grid B. The cell nuclei are stained blue with Hoechst and the red represents the cell skeletons (β-tubulin antibody). Bar is 100 μm

Fig. 3 Orientation of the cells and nuclei on 1D periodic structures after a 4 day culture. The fluorescent staining of the nuclei with Hoechst (**a**) and of the entire cells with SYBR orange protein stain (**b**) shows that the nuclei are also orientated. While the quantification is more easily done from the pictures with nuclei staining, **c** shows the degree of orientation of the cell nuclei on 12.5 μm (*black*) and 25 μm (*dark gray*) and on smooth steel (*light gray*). The percentage of the cell nuclei (Y-axis), whose orientation diverged less than 2, 2.5, 3, 3.5, 5, 10, 20 and 45 ° was calculated using the CellProfiler program. For random orientation, 50 % is reached at 45. Bars in **a** and **b** 100 μm
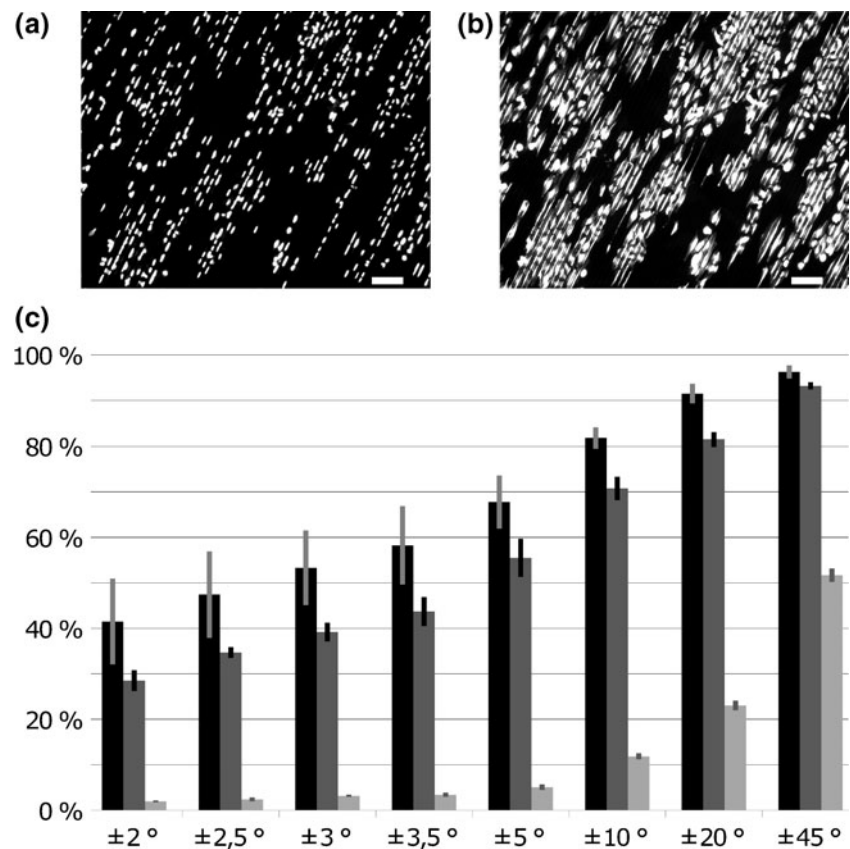
fulfil these conditions. Typical metal structures are shown in Fig. 1a-c. For the 2D metal gratings with 15 μm periodicity and approximately 8 μm in depth (Fig. 1a), we measured a contact angle of 150 °, which can be considered as highly hydrophobic, while a clean and polished steel surface showed a contact angle of only 80 °. The structure (Fig. 1a) was replicated to PC (Fig. 1d) and the contact angle remained unchanged (150 °). The hydrophobicity is caused by spikes which are formed in cross points where ablated lines cross and holes are formed in combination with the self-formed nanostructures.

Another type of structure is seen in Fig. 1b. These coral-like structures are self-organized and the size of their average structural formation is dependent from the laser fluence. The micron structure is again covered with the laser induced nanoscale structures. In contrast to polished and clean metal, this pseudo-periodic, coral-like structure showed, at first, a more hydrophilic nature with a contact angle of 30 °, but interestingly, in the course of time, it turned to 170 °, presumably because of interaction with the carbon dioxide of the air (Kietzig et al. 2009). The contact angle of the structure was decreased to 150 ° when replicated to PC (Fig. 1e) (while for 2D periodic gratings, the contact angle remained unchanged). One possible explanation for this difference is that the micron level features of the positive coral structure is similar with those of its negative copies,

while in the case of 2D gratings, the positive and the negative structures are different in this level. Another possible explanation lies in the nanostructures; in their formation and arrangement (e.g., LIPPS orientation).

In addition to the grid and coral structures, several linear structures were manufactured. A typical linear grating employed in the cell cultures is shown in Fig. 1c, while Fig. 1f represents a crossing point of two linear gratings replicated on PC. As seen in Fig. 1, hot embossing processes result in imprints with well-formed details.

3.2 Control of cell behaviour

To test the biological properties of these structures, cells were grown on the patterns of both steel and PC. All substrates were pre-wetted in a complex media for several hours. This was done to weaken the effects of extreme wettabily and its possible effects on cell locations at the initial stage (via cell drifting with fluid/gas movements on capillary structures at the start). A structure on stainless steel (Fig. 2) greatly altered the cell morphology after two days of culture. The cells were highly elongated and aligned with the grooves in the steel, while on the smooth surfaces, the cells exhibited a typical flatten and spread, plate-like shape (Fig. 2). On these grating structures, the cytoskeleton (and cytosol) of the cells was located even in a single groove. In
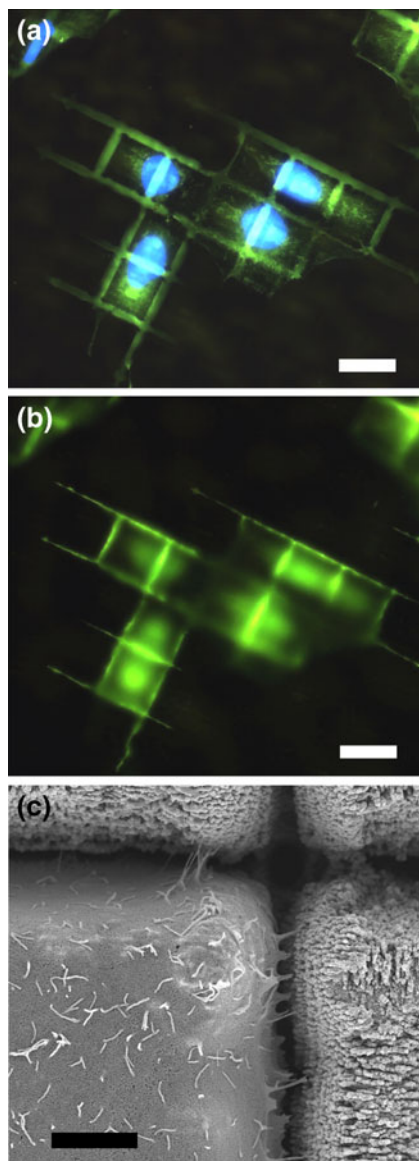
Fig. 4 Cell morphologies on a grid structure after a 2 day culture. **a** Fluorescence microscope image of the cells when the focal plane is on the top of the structure. **b** Focal plane is ten microns below the one in A. **c** Scanning electron microscope image of cells growing downwards. Bars **a** 25 μm, **b** 25 μm and **c** 4 μm

addition, the results indicate that the location of the cells could be controlled on sparse grating as well, such as on the formations in the borderlands of the actual gratings of interest (suppl. Fig. 1). This is possibly due to slower migration rates or increased adhesion on the structures.

3.2.1 Cell growth on linear grating structures

The effect of the width of the period to cell orientation is demonstrated in this study by comparing two different widths (12.5 μm and 25 μm) with the smooth steel surface as the control. On the control surface, the cell nuclei orientated randomly as expected, while on the structure with 12.5 μm periodicity practically all of the cell nuclei, excluding those of dividing cells, were elongated and aligned with the structure (Fig. 3a). These nuclei of post-mitotic cells can be seen as pairs of condensed but adjacent bright "dots" with rounder shapes. Similarly, in a protein staining, freshly divided cells have a brighter emission (Fig. 3b). However, the quantification of the aligned cells was problematic because of the confluence of the cells after a four day culture. Hence, the orientation of the nuclei was measured instead (Fig. 3c). When the period was raised to 25 μm, the number of highly orientated nuclei decreased, which can be explained by an increase in spatial freedom to cells. Note that a typical human somatic cell nucleus has a diameter of 5–10 μm. The control surface reached an orientation level of 50 % at ±45 ° as expected, while the difference between the two grating structures decreased. In neither case, the linear grating structures on the steel plates did not affect the proliferation rates notably when compared with the flat surface.

3.2.2 Filopodial growth on positive and negative structures

The fluorescent immuno-staining with a specific antibody shows that the long extension seen in Fig. 2 includes tubulin fibres. On the steel plates, the filopodial growth cannot be seen in the SEM images, since the cell protrusions are located deep in the grooves. However, analysis by fluorescence microscopy reveals that the cells protrude in the grooves and elongate along them (Fig. 4). Contrary to the growth on the steel plates, on the complementary micron scale structure with a negative topography, the cells grow upon narrower ridges and filopodia grow along the top of the structure (Fig. 5a-d). Figure 5d shows an example of such a filopodium growing on PC. It needs to be reminded here that because the structures on PC are negative imprints of those on steel, grooves on the steel plates become ridges on PC and their size changes accordingly.

3.2.3 Cell growth on quasiperiodic structures

Contrary to linear structures, which had no significant effect on proliferation, the growth of the U2OS cells was clearly inhibited on the quasi- or pseudo-periodic coral structures (Fig. 5 and suppl. Fig. 2). The growth rate was decreased by 78.6±9.9 % compared to the cells grown on the flat surface. As portrayed by Fig. 5e, f, cell morphology is now more condensed and the cells form groups where the nuclei are close to each other. Moreover, the cells seem to have more contact deeper into the pits of the structures with their filopodia, which was not as commonly observed in other types of structures on PC.
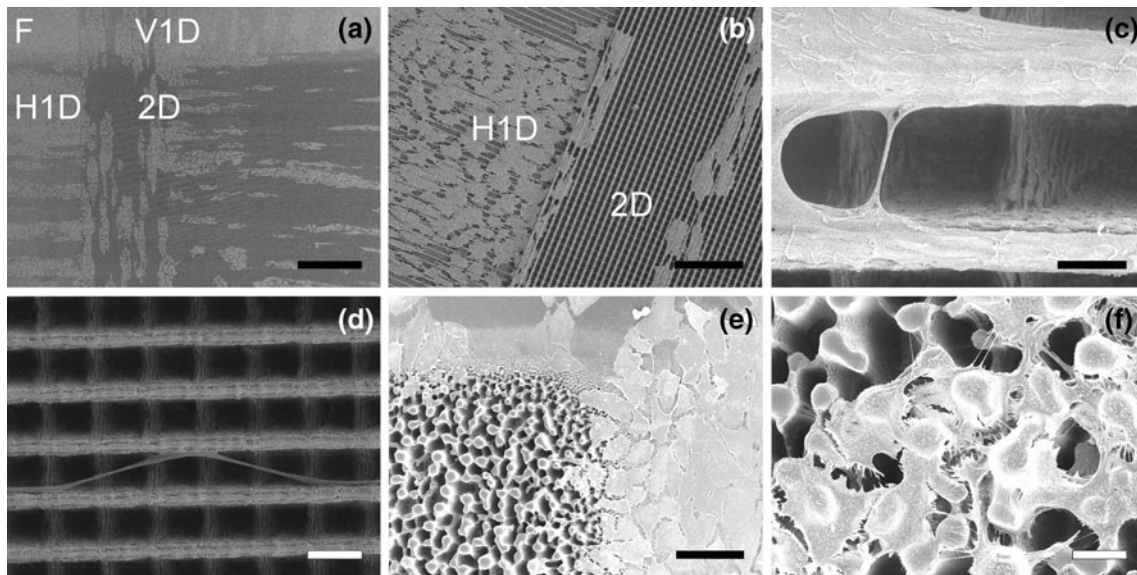
Fig. 5 Cell cultures on plastic replicas. **a** In the upper-left corner of the image (area F), confluent cells can be seen on the smooth surface after a 4 day culture, while on the upper and left margins there are "vertical" (area V1D) and "horizontal" 1D (area H1D) grating structures, respectively, which cross elsewhere in the picture (2D). **b** Horizontal structures (H1D in A) and 2D grid (2D in A). **c, d** Details of the grid structure can be seen down left in A (area 2D in A). **e, f** Cells on smooth and on coral-like structures. Bars **a** 1 mm, **b** 100 μm, **c** 4 μm, **d** 10 μm, **e** 100 μm and **f** 20 μm

4 Discussion

4.1 Relation to previous studies

Other studies carried out using different manufacturing methods confirm that certain structural dimensions can alter the behaviour of cells—although some effect can be specific to the cell type, cell line or tissue. For example, the combination of nano- and microstructures resembling tissue matrixes, nanosized nodules of TiO_2 around 300 nm in diameter, located in micron sized pits, has been found to be a good target for osteoblast (Kubo et al. 2009). On the plastic substrates, PC (Rebollar et al. 2008) and polystyrene (Zhu et al. 2004), the cells have been found to align with nanogrooves and ridges, again with the same size of a few hundred nanometres. In the present study, the cells aligned with 12.5 and 25 μm sized periodic structures, in which various nanostructures located on the ridges and grooves with a structural dimension down to and below 100 nm. A possible explanation is that the size of the structures is in the same scale than the size of the individual cells, cell organelles and proteins, and protein complexes (e.g., focal adhesion proteins, integrin). Hence, the topographical patterns represented in this study may help in the development of implantable devices— when applied directly to surfaces of metallic devices (electrodes, screws, etc.) adhesion and contact could be improved or used as a mould for plastic devices.

4.2 Orientation of the cells

A study by Fujita et al. (Fujita et al. 2009) on cell alignment on nanogrooved substrates suggests the importance of the retraction phase of the cell protrusions. The study suggests that slower retraction parallel to grooves could lead cells to align with the nanogrooves. In the case of hierarchical periodic structures made by laser ablation, the submicron structures or "nanogrooves" can be orientated either parallel or perpendicular in relation to higher structural levels (Fig. 2). This attribute, a property of LIPPS, can be controlled by the laser polarization angle relative to the ablated line direction and by the fluence and pulse number. Nevertheless, it seems that the studies referred to here— including the study by Fujita et al.—agree that the filopodia "grows" or retains parallel to the nanogrooves, which eventually lead cells to elongate with the nanogroove direction. In the present study, this was seen on the bottom of the micron scale grooves of the metallic grating structures, and on the corresponding area (on the top of the ridges) of the negative plastic copies. Hence, the high degree of cell orientation (seen in the present study) may be due to the cumulative effect of the parallel orientations of both nanometre and micron scale structural cues.

4.3 Inhibition and morphology on quasiperiodic structures

The inhibitory effect was predominant on the non-continuous "coral-like" structures. Similarly, Schlie et al.

(2009) report inhibitory and selective properties of spike structures generated using the same technique. Furthermore, Alves et al. (2009) found superhydrophobic poly-L-lactic acid surfaces to posses similar inhibitory effects, and even to be able to control the proliferation of bone marrow-derived cells. Thus, these kinds of structures could be useful in designing selective platforms for the cells. By laser ablation, such inhibitory "zones" can be easily designed and manufactured (an example of this is shown in the supplementary figures). Furthermore, the zone or line width can be adjusted to be as narrow as only few microns and can be copied to plastic with extremely high aspect ratios resembling more natural 3D matrixes. It is worth mentioning herein that while the hydrophobic multilevel structures (like in the present study) may inhibit the growth of osteoblastic cells in general, similar but hydrophilic structures may improve both proliferation and differentiation (Zhao et al. 2011). Hence, these coral-like structures imprinted on a hydrophilic surface or with an appropriate hydrophilic surface modification could be good targets for osteoblasts as well.

In a recent study, the deformability of cancerous cell lines was evaluated (Davidson et al. 2010). In this case, the cell nuclei on pillars underwent deformations of the nuclei. Interestingly, on the coral structures of the present study, the cells had a slower proliferation rate but highly branched cell morphology. This could indicate that structural features may decrease the deformability of cancerous cells. Naturally, it should be taken into account whether cancerous cells change their gene expression or show other signs of specialization than merely the changes in their morphology. However, further research exploring primary cell lines would be significant in this regard. Recently, Brammer et al. (2011) found hydrophobic nanopillars useful in controlling the differentiation of mesenchymal stem cells, further highlighting the importance of structural cues and surface energies in the cell fate and hence in the material design for life-science purposes. Laser ablation can provide very fast ways to produce a variety of nanostructures with different surface energies.

4.4 Method properties and future directions

Another interesting direction for future research would be to study the effects of various LIPPS signatures and their orientation. The theory of LIPPS formation is relatively well known (Qi et al. 2009; Zhao et al. 2007) and LIPPS can be controlled with, for example, polarization and the angle of incidence. Wang et al. (2008) generated LIPPS to polystyrene with a p-polarized laser using a wavelength of 266 nm. They found these structures effective in the control of cell migration and orientation. However, the study presents only the effects of nanostructures, while micron sized structural

formations are absent. Additionally, high laser fluence can induce chemical modifications to the surface, which can be desirable in various biomedical purposes. Furthermore, laser ablation can also be carried out in liquid ambiences (Chung et al. 2010; Yang et al. 2009), which can affect structural formations as well, and induce complex chemical modifications in a single step. It could also allow simultaneous and immediate mineralization processes of the laser ablated surface in the presence of suitable additives (Tavangar et al. 2011).

In addition, laser ablation provides certain advantages over other nano- and micro patterning techniques. It can be applied directly on a variety of materials and without any contact to them. It is capable of producing both micro- and nano features in a single step. It can also be applied on irregular topographies or heterogeneous surfaces, and on both soft and hard materials—all of which are important aspects in biomaterial design (Balasundaram et al. 2006). It allows direct modification of soft material—useful for, for example, generating 3D matrixes in collagen (Liu et al. 2005)—or indirect modification by imprinting structures to plastics as in the present study. It is applicable to both opaque and transparent materials, and in the latter case, it can produce structures even inside the material (Kanehira et al. 2005; Liu et al. 2005) or under a transparent sealing—not to mention that it is powerful for welding as well—even glass (Chung et al. 2010). Furthermore, laser ablation is capable of making structures with an extremely high aspect ratio and deep holes with nanoscale decoration (Huang et al. 2009), which could be used as a scaffold for capillary system, for instance. Laser ablation is easy to use for macroscopic designing of the mould and it allows endless modifications by changing the optical set up, and with multiple beams, the variety of structures is further increased. We also believe that the high flexibility of the technique could be a response to the challenges of interface tissue engineering (Seidi et al. 2011) or provide novel scaffolds for studying cultured neuronal networks.

5 Conclusions

Femtosecond laser ablation is able to produce multi-level periodic structures. It is tuneable and can hence be used to design structures that affect certain cell types or lines. It is versatile and can be applied even on irregular surfaces. Furthermore, it is able to handle diverse materials and alter their physico-chemical properties. In addition to control over the cell shape or proliferation, it can also be used to control the cell location on the substrate. Structures can be imprinted on common plastics, and hence mass production of culture plates or other biomedical plastic products becomes possible. This study concludes that it can be used

to control cell migration and localization, morphology, spreading, orientation and proliferation. Especially the orientation of U2OS cells was fully controlled in this study on both steel and plastic replicas.

References

N.M. Alves, J. Shi, E. Oramas, J.L. Santos, H. Tomas, J.F. Mano, Bioinspired superhydrophobic poly(L-lactic acid) surfaces control bone marrow derived cells adhesion and proliferation. J. Biomed. Mater. Res. A. **91**, 480–488 (2009)

G. Balasundaram, T.J. Webster, Nanotechnology and biomaterials for orthopedic medical applications. Nanomedicine (London) **1**, 169–176 (2006)

K.S. Brammer, C. Choi, C.J. Frandsen, S. Oh, S. Jin, Hydrophobic nanopillars initiate mesenchymal stem cell aggregation and osteo-differentiation. Acta. Biomater. **7**, 683–690 (2011)

C.K. Chung, H.C. Chang, T.R. Shih, S.L. Lin, E.J. Hsiao, Y.S. Chen, E.C. Chang, C.C. Chen, C.C. Lin, Water-assisted CO(2) laser ablated glass and modified thermal bonding for capillary-driven bio-fluidic application. Biomed. Microdevices. **12**, 107–114 (2010)

P.M. Davidson, O. Fromigue, P.J. Marie, V. Hasirci, G. Reiter, K. Anselme, Topographically induced self-deformation of the nuclei of cells: dependence on cell type and proposed mechanisms. J. Mater. Sci. Mater. Med. **21**, 939–946 (2010)

J. El Ali, P.K. Sorger, K.F. Jensen, Cells on chips. Nature **442**, 403–411 (2006)

S. Fujita, M. Ohshima, H. Iwata, Time-lapse observation of cell alignment on nanogrooved patterns. J. R. Soc. Interface. **6**(Suppl 3), S269–S277 (2009)

M. Huang, F. Zhao, Y. Cheng, N. Xu, Z. Xu, Large area uniform nanostructures fabricated by direct femtosecond laser ablation. Opt. Express **16**, 19354–19365 (2008)

Y. Huang, S. Liu, W. Li, Y. Liu, W. Yang, Two-dimensional periodic structure induced by single-beam femtosecond laser pulses irradiating titanium. Opt. Express **17**, 20756–20761 (2009)

N. Huebsch, D.J. Mooney, Inspiration and application in the evolution of biomaterials. Nature **462**, 426–432 (2009)

T.R. Jones, I.H. Kang, D.B. Wheeler, R.A. Lindquist, A. Papallo, D.M. Sabatini, P. Golland, A.E. Carpenter, Cell Profiler Analyst: data exploration and analysis software for complex image-based screens. BMC Bioinforma. **9**, 482 (2008)

S. Kanehira, J. Si, J. Qiu, K. Fujita, K. Hirao, Periodic nanovoid structures via femtosecond laser irradiation. Nano. Lett. **5**, 1591–1595 (2005)

A.M. Kietzig, S.G. Hatzikiriakos, P. Englezos, Patterned superhydrophobic metallic surfaces. Langmuir **25**, 4821–4827 (2009)

K. Kubo, N. Tsukimura, F. Iwasa, T. Ueno, L. Saruwatari, H. Aita, W.A. Chiou, T. Ogawa, Cellular behavior on TiO2 nanonodular structures in a micro-to-nanoscale hierarchy model. Biomaterials **30**, 5319–5329 (2009)

J.Y. Lim, H.J. Donahue, Cell sensing and response to micro- and nanostructured surfaces produced by chemical and topographic patterning. Tissue Eng. **13**, 1879–1891 (2007)

Y. Liu, S. Sun, S. Singha, M.R. Cho, R.J. Gordon, 3D femtosecond laser patterning of collagen for directed cell attachment. Biomaterials **26**, 4597–4605 (2005)

W.A. Loesberg, J. te Riet, F.C. van Delft, P. Schon, C.G. Figdor, S. Speller, J.J. van Loon, X.F. Walboomers, J.A. Jansen, The threshold at which substrate nanogroove dimensions may influence fibroblast alignment and adhesion. Biomaterials **28**, 3944–3951 (2007)

A. Mata, C. Boehm, A.J. Fleischman, G. Muschler, S. Roy, Analysis of connective tissue progenitor cell behavior on polydimethylsiloxane smooth and channel micro-textures. Biomed. Microdevices. **4**, 267–275 (2002)

Y. Mei, M. Goldberg, D. Anderson, The development of high-throughput screening approaches for stem cell engineering. Curr. Opin. Chem. Biol. **11**, 388–393 (2007)

U. Meyer, A. Buchter, H.P. Wiesmann, U. Joos, D.B. Jones, Basic reactions of osteoblasts on structured material surfaces. Eur. Cell. Mater. **9**, 39–49 (2005)

N.E. Paul, C. Skazik, M. Harwardt, M. Bartneck, B. Denecke, D. Klee, J. Salber, G. Zwadlo-Klarwasser, Topographical control of human macrophages by a regularly microstructured polyvinylidene fluoride surface. Biomaterials **29**, 4056–4064 (2008)

S. Puckett, R. Pareta, T.J. Webster, Nano rough micron patterned titanium for directing osteoblast morphology and adhesion. Int. J. Nanomedicine. **3**, 229–241 (2008)

L. Qi, K. Nishii, Y. Namba, Regular subwavelength surface structures induced by femtosecond laser pulses on stainless steel. Opt. Lett. **34**, 1846–1848 (2009)

D. Qin, Y. Xia, G.M. Whitesides, Soft lithography for micro- and nanoscale patterning. Nat. Protoc. **5**, 491–502 (2010)

E. Rebollar, I. Frischauf, M. Olbrich, T. Peterbauer, S. Hering, J. Preiner, P. Hinterdorfer, C. Romanin, J. Heitz, Proliferation of aligned mammalian cells on laser-nanostructured polystyrene. Biomaterials **29**, 1796–1806 (2008)

J.B. Recknor, D.S. Sakaguchi, S.K. Mallapragada, Directed growth and selective differentiation of neural progenitor cells on micro-patterned polymer substrates. Biomaterials **27**, 4098–4108 (2006)

U. Reich, P.P. Mueller, E. Fadeeva, B.N. Chichkov, T. Stoever, T. Fabian, T. Lenarz, G. Reuter, Differential fine-tuning of cochlear implant material-cell interactions by femtosecond laser microstructuring. J. Biomed. Mater. Res. B. Appl. Biomater. **87**, 146–153 (2008)

K. Sato, Y. Tanaka, B. Renberg, T. Kitamori, Combining microchip and cell technology for creation of novel biodevices. Anal. Bioanal. Chem. **393**, 23–29 (2009)

S. Schlie, E. Fadeeva, J. Koch, A. Ngezahayo, B.N. Chichkov, Femtosecond Laser Fabricated Spike Structures for Selective Control of Cellular Behavior. J. Biomater. Appl. (2009)

R.C. Schmidt, K.E. Healy, Controlling biological interfaces on the nanometer length scale. J. Biomed. Mater. Res. A. **90**, 1252–1261 (2009)

A. Seidi, M. Ramalingam, I. Elloumi-Hannachi, S. Ostrovidov, A. Khademhosseini, Gradient biomaterials for soft-to-hard interface tissue engineering. Acta. Biomater. **7**, 1441–1451 (2011)

A. Tavangar, B. Tan, K. Venkatakrishnan, Synthesis of bio-functionalized three-dimensional titania nanofibrous structures using femtosecond laser ablation. Acta. Biomater. **7**, 2726–2732 (2011)

P.J. ter Brugge, S. Dieudonne, J.A. Jansen, Initial interaction of U2OS cells with noncoated and calcium phosphate coated titanium substrates. J. Biomed. Mater. Res. **61**, 399–407 (2002)

V.N. Truskett, M.P. Watts, Trends in imprint lithography for biological applications. Trends Biotechnol. **24**, 312–317 (2006)

G.H. Underhill, S.N. Bhatia, High-throughput analysis of signals regulating stem cell fate and function. Curr. Opin. Chem. Biol. **11**, 357–366 (2007)

P. Uttayarat, G.K. Toworfe, F. Dietrich, P.I. Lelkes, R.J. Composto, Topographic guidance of endothelial cells on silicone surfaces with micro- to nanogrooves: orientation of actin filaments and focal adhesions. J. Biomed. Mater. Res. A. **75**, 668–680 (2005)

A.Y. Vorobyev, C. Guo, Laser turns silicon superwicking. Opt. Express **18**, 6455–6460 (2010)

X. Wang, C.A. Ohlin, Q. Lu, J. Hu, Cell directional migration and oriented division on three-dimensional laser-induced periodic surface structures on polystyrene. Biomaterials **29**, 2049–2059 (2008)

Y. Yang, J. Yang, C. Liang, H. Wang, X. Zhu, N. Zhang, Surface microstructuring of Ti plates by femtosecond lasers in liquid ambiences: a new approach to improving biocompatibility. Opt. Express **17**, 21124–21133 (2009)

W.Y. Yeong, H. Yu, K.P. Lim, K.L. Ng, Y.C. Boey, V.S. Subbu, L.P. Tan, Multiscale Topological Guidance for Cell Alignment via Direct Laser Writing on Biodegradable Polymer. Tissue. Eng. Part. C. Methods. (2010)

R.N. Zare, S. Kim, Microfluidic platforms for single-cell analysis. Annu. Rev. Biomed. Eng. **12**, 187–201 (2010)

X. Zhang, F. Shi, J. Niu, Y. Jiang, Z. Wang, Superhydrophobic surfaces: from structural control to functional application. J. Mater. Chem. **18**, 621–633 (2008)

Q.Z. Zhao, S. Malzer, L.J. Wang, Formation of subwavelength periodic structures on tungsten induced by ultrashort laser pulses. Opt. Lett. **32**, 1932–1934 (2007)

C. Zhao, P. Cao, W. Ji, P. Han, J. Zhang, F. Zhang, Y. Jiang, X. Zhang, Hierarchical titanium surface textures affect osteoblastic functions. J. Biomed. Mater. Res. A. **99**, 666–675 (2011)

B. Zhu, Q. Zhang, Q. Lu, Y. Xu, J. Yin, J. Hu, Z. Wang, Nanotopographical guidance of C6 glioma cell alignment and oriented growth. Biomaterials **25**, 4215–4223 (2004)